Available online at www.sciencedirect.com
ScienceDirect
Journal of Chromatography B, 852 (2007) 562–570
JOURNAL OF CHROMATOGRAPHY B
www.elsevier.com/locate/chromb

Separation and mass spectrometric characterization of covalently bound skin ceramides using LC/APCI-MS and Nano-ESI-MS/MS

Hany Farwanah[a,1], Barbara Pierstorff[a,1], Christian E.H. Schmelzer[b,2], Klaus Raith[b,2], Reinhard H.H. Neubert[b,2], Thomas Kolter[a,1], Konrad Sandhoff[a,*]

[a] *LIMES – Life and Medical Sciences Bonn, Program Unit Membrane and Lipid Biochemistry, Laboratory of Biology & Lipid Biochemistry, Friedrichs-Wilhelm-University, Gerhard-Domagk-Str. 1, D-53121 Bonn, Germany*
[b] *Institute of Pharmacy, Martin Luther University Halle-Wittenberg, Wolfgang-Langenbeck-Str. 4, D-06120 Halle (Saale), Germany*

Received 15 November 2006; accepted 12 February 2007
Available online 24 February 2007

Abstract

Ceramides covalently bound to keratinocytes are essential for the barrier function of the skin, which can be disturbed in diseases, such as psoriasis and atopic dermatitis. These ceramides of the classes ω-hydroxyacyl-sphingosine and ω-hydroxyacyl-6-hydroxysphingosine contain an ω-hydroxy fatty acid. For their separation and identification, a new analytical approach based on normal phase liquid chromatography coupled to atmospheric pressure chemical ionization mass spectrometry and tandem nano-electrospray mass spectrometry, respectively, is presented here. Tandem mass spectrometry provided structural information about the sphingoid base as well as the fatty acid moieties. The chain lengths of the bases ranged from C12 to C22, the chain lengths of the fatty acids varied between C28 and C36. In total, 67 ceramide species have been identified in human skin. The analytical methods presented in this work can be helpful for investigating alterations in the ceramide composition of the skin as seen in psoriasis, atopic dermatitis, and diseases with impaired epidermal barrier function.

Keywords: Skin; Covalently bound ceramides; LC/APCI-MS; Nano-ESI-MS/MS

1. Introduction

The stratum corneum (SC) as the outermost layer of the skin has a barrier function and protects the organism against environmental influences and transepidermal water loss. Its unique morphology consists of keratin-enriched corneocytes embedded in a distinctive mixture of lipids that contains mainly ceramides, free fatty acids, and cholesterol [1,2]. These intercellular lipids can be easily extracted with organic solvents. The corneocytes are surrounded by a network of highly cross-linked proteins, the so-called cornified envelope (CE) [3,4]. ω-Hydroxy ceramides, ω-hydroxy fatty acids, and eventually also fatty acids are covalently attached to proteins of the CE [1,5]. They can be liberated and extracted only after mild alkaline hydrolysis [5].

Among the skin lipids, ceramides are known to play a crucial role in the SC. Structurally, they belong to the class of sphingolipids and consist of long chain sphingoid bases (LCB) linked to long chain fatty acids (FA) via an amide-bond. In SC ceramides, three types of sphingoid bases occur. These sphingoid bases are sphingosine (S), phytosphingosine (P), and 6-hydroxysphingosine (H). The amide-linked fatty acids can be α-hydroxylated (A) or non-hydroxylated (N). In addition, the ω-hydroxy fatty acids (O) can be esterified with another fatty acid (E) or attached covalently to the CE. According to the nomenclature suggested by Motta et al. [6] and Robson et al. [7], the designation of a certain ceramide class results from the combination of a letter representing the type of the fatty acid and another one representing the type of the sphingoid base. Nine classes of free extractable ceramides have been discovered: Cer [EOS], Cer [NS], Cer [AS], Cer [EOP], Cer [NP], Cer [AP], Cer [EOH], Cer [NH], and Cer [AH]. The CE ceramide classes known to date are ω-hydroxyacyl-sphingosine (Cer [OS]) and ω-hydroxyacyl-6-hydroxysphingosine (Cer [OH]). The existence of Cer [OP] has been previously assumed, but not confirmed

* Corresponding author. Tel.: +49 228 735346; fax: +49 228 737778.
E-mail address: sandhoff@uni-bonn.de (K. Sandhoff).
[1] Tel.: +49 228 735346; fax: +49 228 737778.
[2] Tel.: +49 345 5525215; fax: +49 345 5527292.

1570-0232/$ – see front matter © 2007 Elsevier B.V. All rights reserved.
doi:10.1016/j.jchromb.2007.02.030

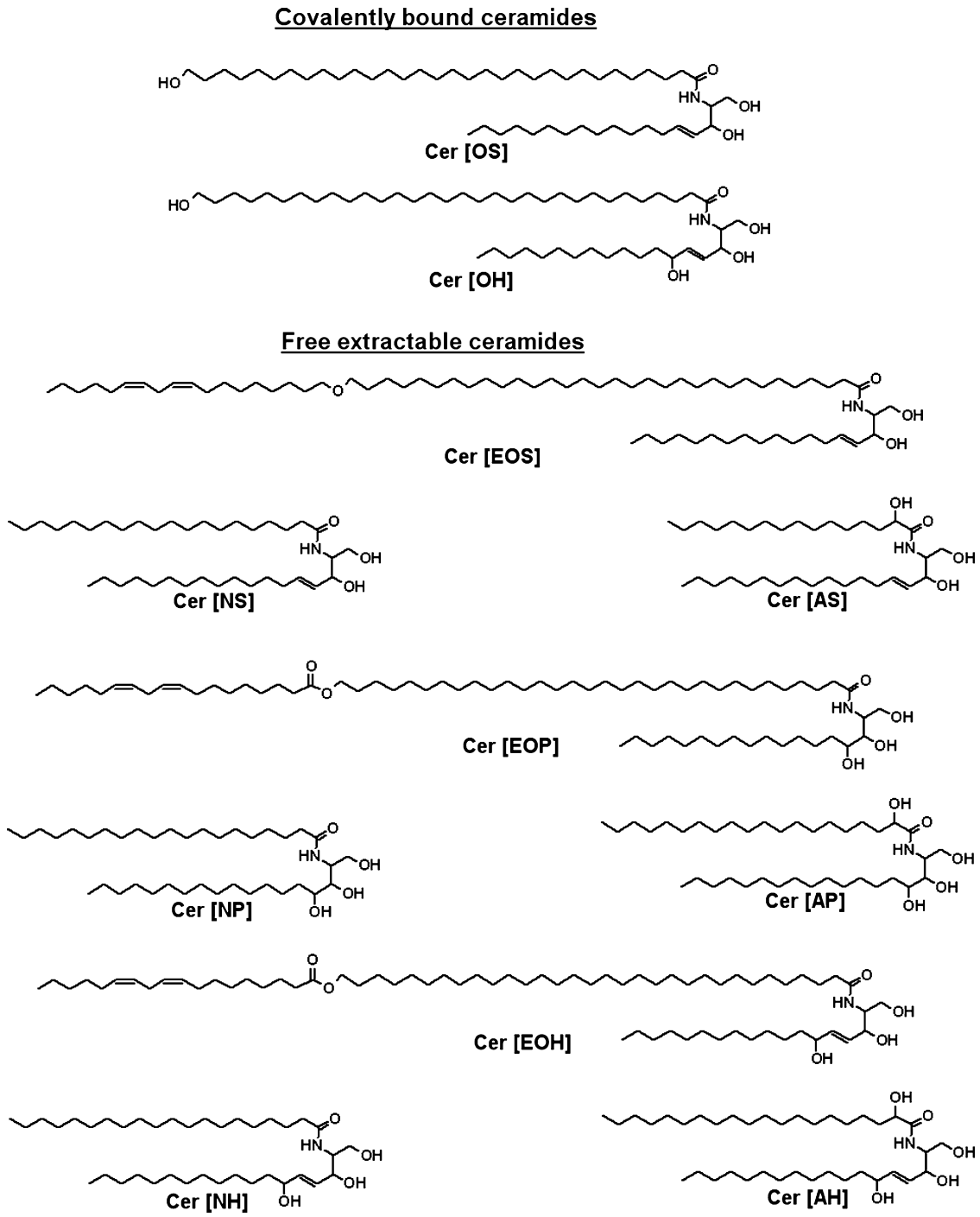

Fig. 1. Structures of representative species for free extractable and covalently human bound skin ceramides.

yet [8]. Fig. 1 shows the structures of the mentioned ceramide classes.

The ω-hydroxy ceramides are ester-linked by their ω-hydroxyl group to proteins of the CE [9–12], where, they are thought to influence the organization of the unbound intercellular lipids [1,9]. In addition, they have been found to be critical for epidermal barrier function and corneocyte cohesion [13,14]. Doering et al. demonstrated a correlation between the covalent attachment of the ω-hydroxy ceramides and the maturation as well as the chemical and the enzymatic resistance of the stratum corneum [12,15,16]. Furthermore, the UVB-induced disruption of the epidermal barrier function has been reported to impair CE ceramides [13]. In addition, Macheleidt et al. showed that a decrease in the CE ceramide level accompanies atopic dermatitis [17].

Most analytical studies on SC ceramides focused on the free extractable, but not on the covalently bound ceramides [18–27]. Thin-layer chromatography (TLC) is still the method of choice for separation and quantification purposes [5,28,29]. After hydrolysis of ceramides, both the fatty acids and the sph-

ingoid bases can be analyzed by gas chromatography (GC) or gas chromatography/mass spectrometry (GC/MS) [5,30]. This approach, however, does not provide information on the combination of the two moieties. Furthermore, the whole procedure including TLC separation, recovery of the ceramide bands, extraction, derivatization, and subsequent GC analysis is demanding. GC/MS of intact ceramides is possible, but has not found widespread use, presumably because of the requirements of derivatization [31].

In contrast, liquid chromatography/mass spectrometry (LC/MS) enables a direct analysis without derivatization. Analysis of free extractable ceramides by means of reversed phase LC/ESI-MS and ESI-MS/MS has been performed by Raith et al. [20], Raith and Neubert [21], and Vietzke et al. [23,24]. Hsu et al. [32] have performed structural studies among others on CE ceramides as lithium adducts by using positive mode ESI-MS/MS under conditions of low energy collisional-activated dissociation. However, they have not determined the whole pattern of the CE ceramides.

Recently, we reported a new approach using normal phase LC/APCI-MS, which allows separation and simultaneous online detection of the molecular species of free extractable intercellular ceramide classes [26,33]. In the present work, we use this approach to analyze the covalently bound ceramides of human skin. For in-depth structural analysis and precise molecular profiling, fragmentation experiments using Nano-ESI-MS/MS have been carried out.

2. Experimental

2.1. Chemicals and reagents

The ceramide species are designated as ω-fatty acid type: ω-fatty acid chain length/sphingoid base type: sphingoid base chain length. Thus, e.g., a ceramide molecule consisting of a C30 ω-hydroxy fatty acid and a C18 sphingosine is named O:30/S:18-Cer. An analogous compound based on 6-hydroxysphingosine is designated as O:30/H:18-Cer.

Cer [EOS] and Cer [NP] were provided by Goldschmidt (Essen, Germany). These synthetic ceramides were O:30/S:18-Cer and N:18/P:18-Cer species, respectively. Cer [EOS] was additionally esterified with linoleic acid at the ω-position of the C30 ω-hydroxy fatty acid.

Silica TLC plates (Kieselgel 60; 20 cm × 10 cm), were supplied by Merck (Darmstadt, Germany). Solvents for extraction, HPTLC and LC/MS purposes were of HPLC grade and were from Baker (Deventer, The Netherlands), Merck (Darmstadt, Germany) and Roth (Karlsruhe, Germany).

2.2. Preparation of stratum corneum

Foreskin samples were obtained from Dr. Thomas Meyer (Praxisklinik-Grevenbroich, Grevenbroich, Germany). The preparation of the SC was performed according to a previous protocol [34]. In brief, foreskin samples were detached from subcutaneous tissue and transferred into a phosphate buffered saline containing 0.5% trypsin. After sonication for 30 min and an overnight incubation at 37 °C, SC was separated from the residual tissue, washed with PBS, and thereafter with water, and lyophilized. Free extractable lipids were removed from SC by extensive extraction with chloroform/methanol (1:1, v/v), until no more lipids could be detected by TLC. To obtain the covalently attached lipids, SC was suspended in a solution containing 1 M KOH in 95 % methanol 2 h at 60 °C for hydrolysis. Afterwards, the solution was neutralized with acetic acid and separated from residual SC-tissue by centrifugation. The pellet was washed with methanol and all supernatants were combined. To purify the extracted lipids from proteins and other hydrophilic components, a phase separation has been carried out as described previously [35]. In brief, the extracted lipids were dissolved in chloroform, methanol, and water (1:2:0.8, v/v/v). Upon changing the solvent composition to (2:2:1.8, v/v/v), an aqueous and a chloroform phase separated, and the lipids in the chloroform phase were analyzed.

2.3. Preparation of the standard ceramide Cer [OS]

Cer [OS] (O:30/S:18-Cer) was obtained by alkaline hydrolysis of ceramide Cer [EOS] using 4 M NaOH. The hydrolysis was necessary to remove the linoleic acid from the ω-position. After incubation time of 3 h at 60 °C the sample was neutralized with acetic acid and purified from salts as described above.

2.4. HPTLC separation of the covalently bound ceramides

Sample application on the HPTLC plates has been carried out automatically by using a Linomat 4 system (Camag, Berlin, Germany). The chromatographic development was performed twice to the top of the plates using a solvent mixture consisting of chloroform, methanol, and acetic acid (190:9:1, v/v/v). After drying, lipid bands were visualized with 10% $CuSO_4$, 8% H_3PO_4(w/v) and heating the plates to 180 °C for 10 min. Then, the plates were scanned by a densitometer CS 9301PC (Shimadzu, Kyoto, Japan). The measurement has been made in reflectance mode at a wavelength of 595 nm. Quantitative results for all ceramides were related to a calibration curve of Cer [NP] (N:18/P:18).

2.5. Ceramide separation and profiling using LC/APCI-MS

The used LC system included an auto sampler AS 3000, a Spectra System P 4000 pump, and a controller SN 4000 (Thermo Electron, San José, CA, USA). The column was a LichroCart (125 mm × 4 mm, 5 μm particle size) filled with Si 60 Lichrospher particles (Merck, Darmstadt, Germany). The separations have been performed as described previously using a gradient from A: chloroform to B: chloroform, *n*-propanol and acetic acid (80:20:2, v/v/v) with a flow rate of 1 ml/min [26].

The LC system was hyphenated to an ion trap mass spectrometer Finnigan LCQ classic (Thermo Electron, San Jose, CA, USA) with an atmospheric pressure chemical ionization source (APCI) in the positive ion mode. The APCI heater was adjusted to 500 °C and the heated capillary to 150 °C.

Nitrogen was utilized as both auxiliary and sheath gas at flow rates of 9 and 1.2 l/min, respectively. The mass analyzer recorded the mass range between *m/z* 700 and 900 in full scan mode.

2.6. Nano-ESI- and Nano-ESI-MS/MS experiments

Static Nano-ESI-MS and Nano-ESI-MS/MS measurements were carried out using a quadrupole time-of-flight (qTOF) mass spectrometer Q-TOF-2™ (Waters Micromass, Manchester, UK) equipped with a Zspray™ source and a nano-electrospray interface. Precoated Nano-ESI glass capillaries have been obtained from DNU (Berlin, Germany). The instrument was calibrated using a mixture of sodium iodide and caesium iodide. Two microliters of the sample solution were loaded into the capillary using microloader pipette tips (Eppendorf, Hamburg, Germany).

The typical operating conditions for the qTOF mass spectrometer were as follows: capillary voltage, 900 V; sample cone voltage, 35 V; and source temperature, 80 °C. The instrument was operated in the negative ion mode. Full scans were performed between *m/z* 50 and 1500. Ceramides of interest were selected manually for further tandem MS experiments using collision induced dissociation (CID). The quadrupole mass filter was set with low mass (LM) and high mass (HM) resolution settings between 10 and 16 (arbitrary units) depending on experimental conditions. Considering the collision gas pressure and the stability of the ceramides to be investigated, the collision energy was varied between 10 and 55 eV.

All mass spectra were recorded in profile mode and processed using MassLynx (version 3.4, Micromass).

3. Results and Discussion

3.1. Separation of the ω-hydroxy ceramides using HPTLC and their densitometric quantification

For analysis of covalently bound ceramides, the free extractable lipids have been extracted quantitatively before hydrolysis and extraction of the CE-lipids. Between these two steps, the extraction efficiency of the unbound lipids has been confirmed using HPTLC as shown in Fig. 2 (lane 2). The separation of the covalently bound lipids resulted in four bands corresponding to Cer [OH], Cer [OS], ω-hydroxy fatty acids, and free fatty acids as demonstrated in lane 1 of Fig. 2. The assignment of lipid class structures to the separated bands is based on comparison of their R_f values with those of commercially available standards, and with the separation patterns of earlier studies [5,8]. The visualized lipid bands have been scanned densitometrically. Quantification of ceramides by densitometry was performed with the aid of a standard curve of Cer [NP], which is known to be suitable for such purposes as reported previously [29]. According to the quantification data, the amount of Cer [OH] (2.2 μg ± 0.4 /mg SC) accounts for 50% of that of Cer [OS] (5.3 ± 0.4 μg/mg SC). This finding is consistent with those of former studies [5]. The amount of the extracted ceramides expressed in μg is related to the weight of the used SC-tissue in mg. The mean values of three determinations ± SD were calculated.

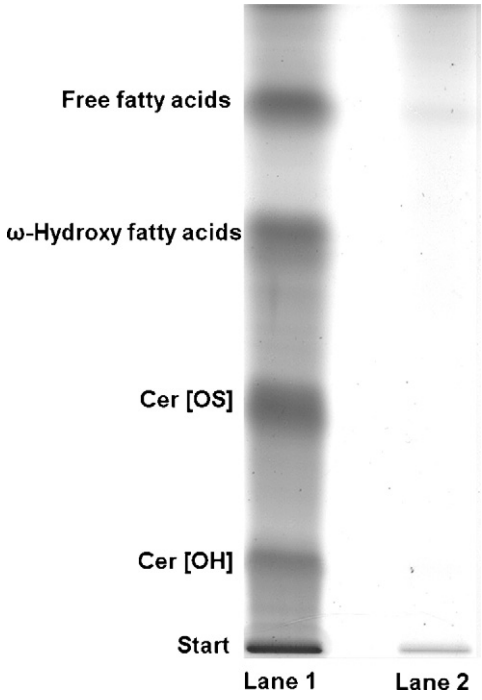

Fig. 2. Separation of SC lipids by means of HPTLC. Lane 1 depicts a chromatogram of the extracted CE lipids including the two ceramide classes Cer [OH] and Cer [OS]. Lane 2 shows that none of the free extractable ceramide classes were present prior to the analysis of the covalently bound lipids.

3.2. Separation of the ω-hydroxy ceramides using LC/APCI-MS

HPTLC is the standard method to separate and quantify the ceramide classes, but the obtainable structural information is limited. The offline hyphenation between HPTLC and the widely used ESI-MS has the disadvantage that polar HPTLC additives suppress often the mass spectrometric signal intensities of interesting ion peaks. Hence, a transfer of the separation pattern obtained by conventional HPTLC to a LC/MS-system with a suitable ionization interface is advantageous. In this context, a normal phase LC/APCI-MS-method has been recently developed allowing the separation of the free extractable SC ceramide classes and the simultaneous online detection of their corresponding species [26,33]. The gradient used enabled a separation pattern, which resembles that of HPTLC procedures [19,26,33]. Based on this concept, the referred LC/APCI-method was applied to separate the covalently bound ceramide classes Cer [OS] and Cer [OH]. Baseline separation and online MS detection have been achieved. Fig. 3 shows a typical chromatogram.

For profiling and structural elucidation purposes, the fractions of Cer [OS] and Cer [OH] were collected according to their corresponding retention times. Thereafter, the fractions were subjected to further analysis by means of Nano-ESI-MS and Nano-ESI-MS/MS. For the sake of clarity, only negative mode Nano-ESI mass profiles will be discussed. Positive mode APCI mass spectra show similar results (data not shown).

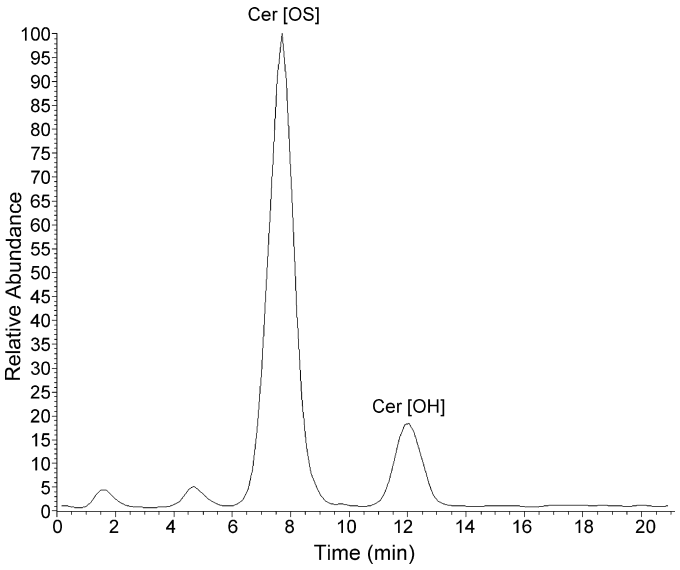

Fig. 3. Chromatogram of the CE ceramide classes Cer [OS] and Cer [OH] as separated by means of normal phase LC coupled to APCI-MS in positive mode. The mass range between *m/z* 700 and 900 was scanned. The detected ions corresponded to those obtained by Nano-ESI-MS in negative full scan mode, which are listed in Table 1.

3.3. Mass spectrometric profiling and structural characterization of the ω-hydroxy ceramides by means of Nano-ESI-MS and Nano-ESI-MS/MS

The mass spectrometric profiles of Cer [OS] and Cer [OH] as obtained by Nano-ESI-MS in negative full scan mode are depicted in Fig. 4. The respective *m/z* values are listed in Table 1. Provided that the chain length of the sphingoid bases is C18 (which is frequently assumed) each of the detected molecular ions would correspond to only one molecular ceramide species. However, fragmentation experiments of each pseudomolecular ion by means of Nano-ESI-MS/MS confirmed a wide structural diversity as demonstrated later on.

Fig. 5 displays a tandem mass spectrum of an authentic standard ceramide O:30/S:18-Cer (*m/z* 748.8). In Fig. 6, proposed pathways for the formation of characteristic fragments related to the amide-linked ω-hydroxy fatty acid (ω-OH-FA) and the long chain sphingoid base (LCB) moieties are illustrated. For each molecular ion, only one of several possible structures is given; alternative structures that correspond to other resonance forms or rearrangement products are omitted for clarity. Accordingly, the structures of ***a***, ***b***, ***c***, ***d***, ***e*** and ***a1***, ***f***, ***e1*** correspond to the pseudomolecular ions $[M\text{-}H]^-$ and $[M\text{-}H\text{-}H_2O]^-$, respectively.

In a cleavage reaction, only one fragment retains the charge and can be detected, whereas the other forms a neutral leaving group. Consequently, the structures of ***a2***, ***b1***, ***c1***, ***d2***, ***e3***, ***f2***, ***f4*** and ***a3***, ***b2***, ***c2***, ***d1***, ***e2***, ***f3*** correspond to the charged and neutral fragments, respectively.

In case of the investigated ceramides, the charge can remain, either on the fatty acid or on the LCB moiety. For example, the direct cleavage of the bond between C2 and C3 yields an ω-OH-FA product ion at *m/z* 508.5 (***b1***), when the charge is retained at the fatty acid moiety. Alternatively, the product ion at *m/z* 237.2 (***d2***), which is characteristic for a C18 sphingosine [24,36], arises.

The neutral loss of one water molecule from the parent ion $[M\text{-}H]^-$ (***a***) can result in the formation of a double bond between C1 and C2 (see ***a1***). The dissociation of the C2–C3 bond in the resulting pseudomolecular ion ***a1*** yields an ω-OH-FA product ion at *m/z* 492.5 (***a2***), which is the most prominent fragment in the spectrum.

The elimination of one water molecule from ***e*** can lead to the formation of a double bond between C2 and C3 (see ***e1*** and ***f***). The cleavage of the N-C2 bond in ***e1*** leads to the formation of a product ion at *m/z* 263.2 (***e3***), which is diagnostic for C18 sphingosine [24,36]. Alternatively, the cleavage of the N-C2 bond in ***c*** results in a characteristic fragment ion for the ω-OH-FA at *m/z* 466.5 (***c1***). On the other hand, a rearrangement of the prod-

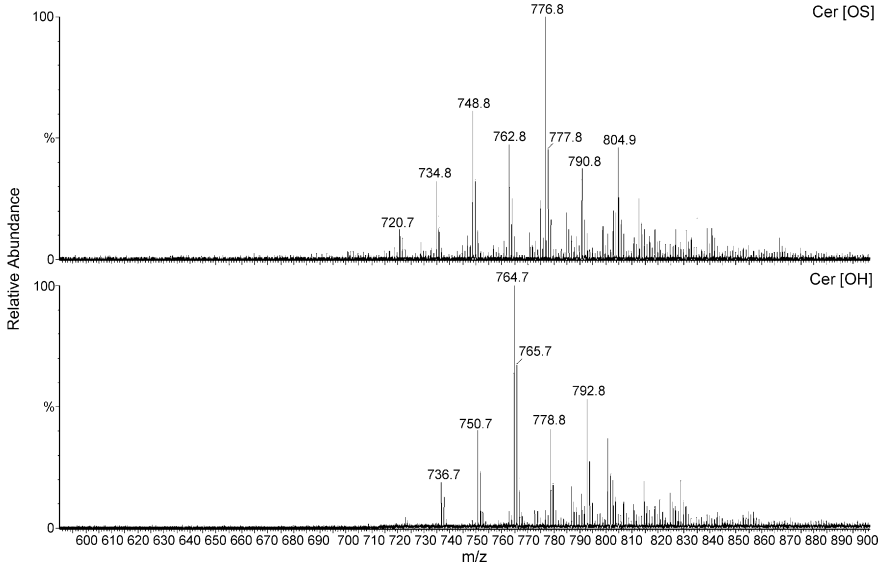

Fig. 4. Mass spectrometric profile $[M\text{-}H]^-$ of Cer [OS] and Cer [OH] as obtained by Nano-ESI-MS in negative full scan mode. The peaks of chloride adducts and ^{13}C isotopes are not designated. Cer [OS] and Cer [OH] were collected according to their retention times in normal phase LC/APCI-MS.

Table 1
Detected variations within the species of Cer [OS] and Cer [OH] as determined by Nano-ESI-MS/MS

Ceramide type	*m/z*	Chain length of the sphingoid base										
		12	13	14	15	16	17	18	19	20	21	22
Chain length of the amide-linked ω-hydroxy fatty acid												
Cer [OS]	720.7					30	29	28				
Cer [OS]	734.8					31	30	29				
Cer [OH]	736.7	34	33	32	31	30	29	28				
Cer [OS]	748.8					32	31	30	29	28		
Cer [OH]	750.7		34	33	32	31	30	29				
Cer [OS]	762.8						32	31	30	29	28	
Cer [OH]	764.7			34	33	32	31	30				
Cer [OS]	776.8					34	33	32	31	30	29	28
Cer [OH]	778.8		36	35	34	33	32	31	30	29		
Cer [OS]	790.8						34	33	32	31	30	29
Cer [OH]	792.8			36	35	34	33	32	31	30		
Cer [OS]	804.8							34	33	32	31	30

uct ion ***f***, which corresponds to $[M\text{-}H\text{-}H_2O]^-$ leads, presumably via an assumed intermediate (***f1***), to the generation of an ω-OH-FA product ion at *m/z* of 467.5 (***f2***), which stands for the C30 ω-OH-FA itself. The fragment ion at *m/z* 449.5 (***f4***) may result from the neutral loss of a water molecule at the omega position of ***f2***.

It is important to emphasize that the product ions at *m/z* 508.5 (***b1***), 492.5 (***a2***), 467.5 (***f2***) and 466.5 (***c1***) are fragments related to the ω-OH-FA and originate from neutral losses of 240.2, 256.2, 281.3 and 282.3, respectively. Using ESI-MS/MS, Han [36] has shown that non-hydroxylated ceramides with C18 sphingosine generate FA product ions with the same neutral losses as mentioned above, together with LBC product ions at *m/z* 237.2 (***d2***) and 263.3 (***e3***), which are diagnostic for ceramide species owing a C18 sphingosine. Our data are consistent with the findings of Han [36] and confirm that the hydroxylation at the omega position of the amide-linked FA does not significantly influence the fragmentation mechanism. This result is also in agreement with previous findings of Hsu et al. [32].

The fragment ions at *m/z* 718.7 and 700.7 in Fig. 5 are of a lesser significance for the identification of the molecular variations within ceramides. They indicate a neutral loss of formaldehyde (Δ*m/z* 30), followed by an additional elimination of one water molecule (Δ*m/z* 18).

The tandem mass spectrum of the standard ceramide O:30/S:18-Cer has been applied to investigate the structural variations within each of the isolated human CE ceramide species (Figs. 7 and 8 and Table 1). The fragmentation spectra of Cer [OS] at *m/z* 720.7 (Fig. 7) and the analogous (Δ*m/z* 16) Cer [OH] at *m/z* 736.7 (Fig. 8) represent examples for such a structural diversity.

In Fig. 7 the product ion at *m/z* 263.2 (***e3***) indicates a C18 sphingosine base (see above), while the intense and characteristic fragment ion at *m/z* 464.4 (***a2***) stands for a C28 ω-OH-FA. Taken together, this indicates the presence of O:28/S:18-Cer, particularly when considering that the total of carbon atoms of the parent ion (*m/z* 720.7) is always 46. Similarly, the product ions of the LCB at *m/z* 235.2 (***e3***) and 249.2 (***e3***) in combination

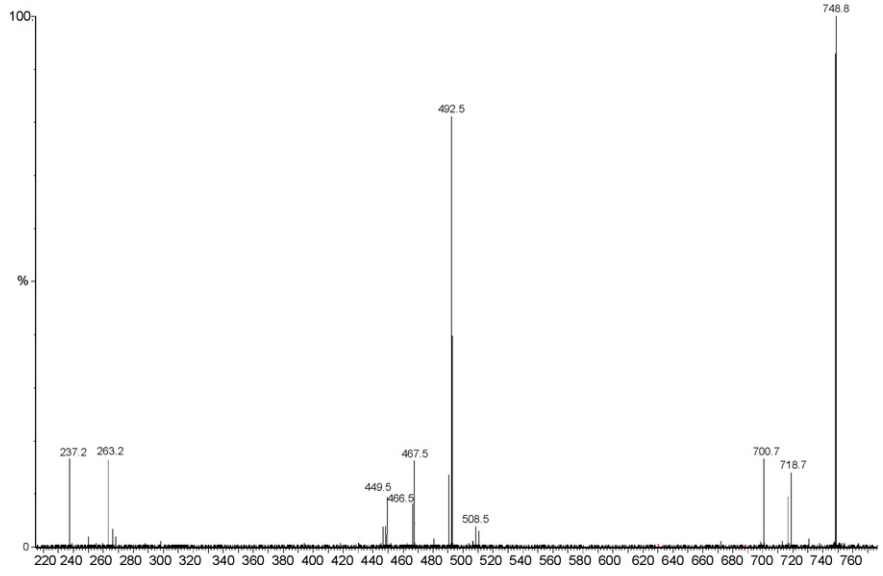

Fig. 5. Fragmentation spectrum of the standard ceramide O:30/S:18-Cer as parent ion with *m/z* 748.8, scan range: 10–850, cycle time: 1.1 s, CID: 35 eV.

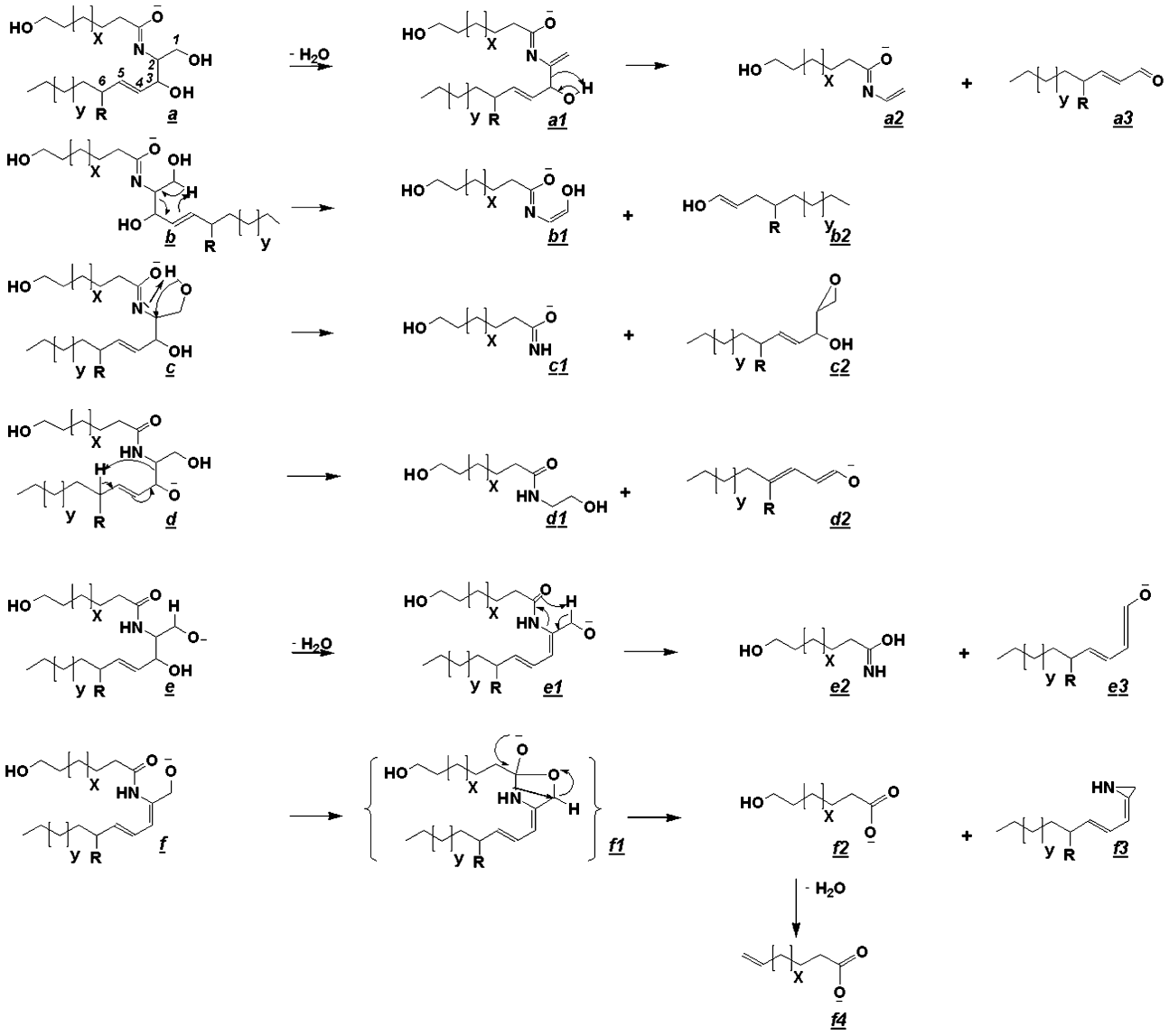

Fig. 6. Suggested pathways for the formation of characteristic fragment ions by means of collision induced dissociation (CID) of Cer [OS] and Cer [OH]. X and Y are equal to 23–31 and 3–13, respectively. R represents H in Cer [OS] and OH in Cer [OH]. In case of the standard ceramide O:30/S:18-Cer, the fragments ***d2*** and ***e3*** are product ions typical for C18 LCB and have *m/z* values of 237.2 and 263.2, respectively. On the other hand, the fragments related to the ω-OH-FA are ***a2***, ***b1***, ***c1***, ***f2***, and ***f4*** with *m/z* values at 492.5, 508.5, 466.5, 467.5, and 449.5, respectively. The formation of (***f2***) from (***f***) is assumed to occur via an intermediate (***f1***). This scheme has been prepared considering previous works of Han [36], Hsu et al. [32], Vietzke et al. [24] and Raith and Neubert [21,22].

with the corresponding ones of the ω-OH-FA at *m/z* 492.5 (***a2***) and 478.4 (***a2***) confirm the occurrence of O:30/S:16-Cer and O:29/S:17-Cer, respectively. These MS/MS data give evidence that distinguishable ceramide homologs are present.

Fig. 8 shows the fragmentation spectrum of a human Cer [OH] with a *m/z* value of 736.7. Here, diagnostic fragments for a C28 ω-OH-FA can be observed at *m/z* 464.4 (***a2***), 439.4 (***f2***), and 421.4 (***f4***), respectively. According to the proposed fragmentation pathway in Fig. 6, parent ions of Cer [OH] are supposed to generate LCB product ions, structurally similar to those of analogous Cer [OS] but with a mass difference of 16 Da originating from the additional 6-hydroxy-function. Since the investigated ceramide species has a C28 ω-OH-FA and a total of 46 carbon atoms, the chain length of the LCB has to be C18. Thus, the *m/z* values of the product ions for the LCB are expected to be 253.2 (=237.2 + 16) (***d2***) and 279.2 (=263.2 + 16) (***e3***), respectively. These LCB product ions have been detected and are depicted in the fragmentation spectrum. Consequently, the combination of the fragmentation data obtained from the ω-OH-FA and LCB confirms the identity of a O:28/H:18-Cer. In addition, the existence of O:29/H:17-Cer and O:30/H:16-Cer is indicated by the typical fragment ions of ω-OH-FA at *m/z* 478.4 (***2a***) and 492.5(***2a***). Further details regarding the detected structural variability of Cer [OS] and Cer [OH] are listed in Table 1.

A remarkable result is that the CE ceramides contain variations with odd-numbered alkyl chain lengths (Table 1) of LCB as well as of ω-OH-FA. This rather unusual finding confirms earlier reports from Wertz et al. [5,37] and Swartzendruber et al. [38] about odd-numbered chain lengths in free extractable as

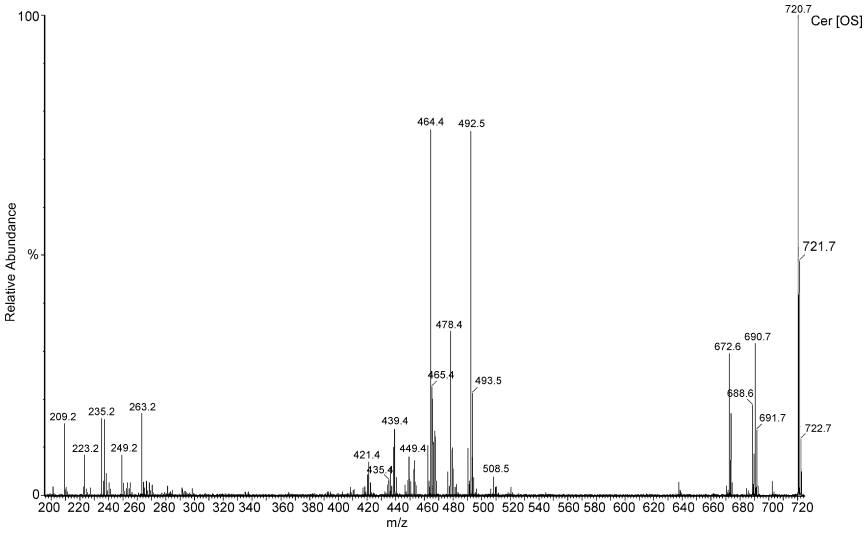

Fig. 7. Fragmentation spectrum of CE Cer [OS] with *m/z* 720.7, scan range: 20–900, cycle time: 1.1 s, CID: 38 eV.

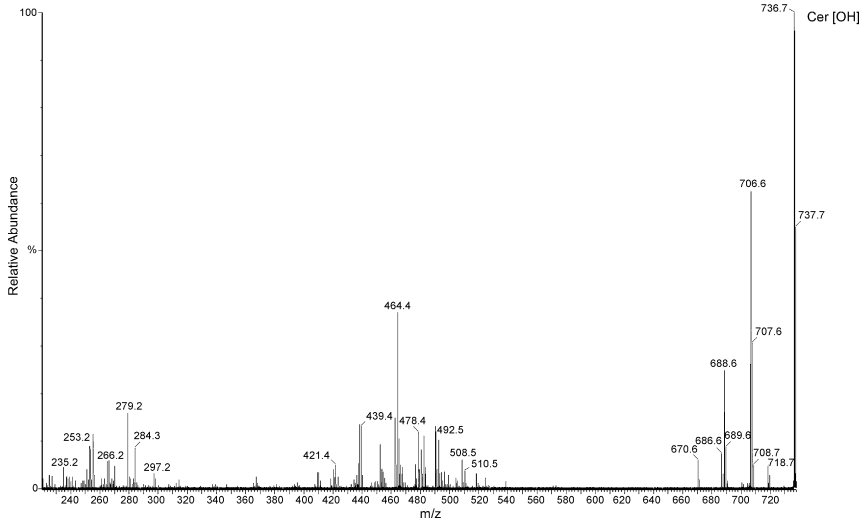

Fig. 8. Fragmentation spectrum of CE Cer [OH] with *m/z* 736.7, scan range: 20–850, cycle time: 1.1 s, CID: 10 eV.

well as in protein bound skin ceramides. Using reversed phase LC/APCI-MS, Masukawa et al. [39] have found free extractable ceramide species with odd-numbered fatty acids ranging from C15 to C27 in human hair. In addition, some of the analyzed ceramides in that study have been reported to contain C17 and C19 sphingoid bases, which were assumed to be branched. Furthermore, Byrdwell and Perry [40] have recently demonstrated that bovine brain contains sphingomyelin and dihydrosphingomyelin species with odd-numbered chain lengths. It is worth mentioning, that no species corresponding to Cer [OP] could be detected in this study, neither by means of LC/APCI-MS nor by means of Nano-ESI-MS. In this context, it has to be kept in mind that the existence of Cer [OP] has been proposed, but not confirmed up to now. In addition, the corresponding free extractable Cer [EOP], which has been recently discovered [41], belongs to the minor ceramide components in the SC. On the other hand, it has to be taken into account that the composition of the SC lipids can be influenced by many factors, such as age, season, gender, anatomical site, as well as inter individual variations [42–44].

4. Conclusions

Recent dermatological research revealed the crucial role of the CE ω-hydroxy ceramides in maintaining the barrier function of the skin. In this work, we showed that a recently reported normal phase LC/APCI-MS method initially developed for separating free extractable ceramides can also be used to separate covalently bound lipids including the two up to date known ceramide classes Cer [OS] and Cer [OH]. The combinatorial structural diversity concerning chain lengths within each of the ceramide classes has been investigated by means of Nano-ESI-MS/MS, and the profiles of the detected species have been compiled. Comparisons of such profiles between healthy and

disordered skin may lead to a better understanding of the underlying molecular mechanisms of such diseases or help to find biomarkers, which can be of a diagnostic value.

Acknowledgments

The authors thank SFB 645 (Sonderforschungsbereich) of DFG (Deutsche Forschungsgemeinschaft) for financial support.

References

[1] K.C. Madison, J. Invest. Dermatol. 121 (2003) 231.
[2] L. Coderch, O. Lopez, A. de la Maza, J.L. Parra, Am. J. Clin. Dermatol. 4 (2003) 107.
[3] A.E. Kalinin, L.N. Marekov, P.M. Steinert, J. Cell Sci. 114 (2001) 3069.
[4] A.E. Kalinin, A.V. Kajava, P.M. Steinert, Bioessays 24 (2002) 789.
[5] P.W. Wertz, K.C. Madison, D.T. Downing, J. Invest. Dermatol. 92 (1989) 109.
[6] S. Motta, M. Monti, S. Sesana, L. Mellesi, R. Ghidoni, R. Caputo, Arch. Dermatol. Res. 130 (1994) 452.
[7] K.J. Robson, M.E. Stewart, S. Michelsen, N.D. Lazo, D.T. Downing, J. Lipid Res. 35 (1994) 2060.
[8] M. Ponec, E. Boelsma, A. Weerheim, Acta Derm. Venereol. 80 (2000) 89.
[9] D.T. Downing, J. Lipid Res. 33 (1992) 301.
[10] M.E. Stewart, D.T. Downing, J. Lipid Res. 42 (2001) 1105.
[11] Z. Nemes, L.N. Marekov, L. Fesus, P.M. Steinert, Proc. Natl. Acad. Sci. USA 96 (1999) 8402.
[12] T. Doering, R.L. Proia, K. Sandhoff, FEBS Lett. 447 (1999) 167.
[13] S. Meguro, Y. Arai, Y. Masukawa, K. Uie, I. Tokimitsu, Arch. Dermatol. Res. 292 (2000) 463.
[14] P.W. Wertz, D.C. Swartzendruber, D.J. Kitko, K.C. Madison, D.T. Downing, J. Invest. Dermatol. 93 (1989) 169.
[15] T. Doering, W.M. Holleran, A. Potratz, G. Vielhaber, P.M. Elias, K. Suzuki, K. Sandhoff, J. Biol. Chem. 274 (1999) 11038.
[16] T. Doering, H. Brade, K. Sandhoff, J. Lipid Res. 43 (2002) 1727.
[17] O. Macheleidt, H.W. Kaiser, K. Sandhoff, J. Invest. Dermatol. 119 (2002) 166.
[18] S. Zellmer, J. Lasch, J. Chromatogr. B 691 (1997) 321.
[19] H. Farwanah, R. Neubert, S. Zellmer, K. Raith, J. Chromatogr. B 780 (2002) 443.
[20] K. Raith, S. Zellmer, J. Lasch, R.H.H. Neubert, Anal. Chim. Acta 418 (2000) 167.
[21] K. Raith, R.H.H. Neubert, Anal. Chim. Acta 403 (2000) 295.
[22] K. Raith, R.H.H. Neubert, Rapid Commun. Mass Spectrom. 12 (1998) 935.
[23] J.P. Vietzke, M. Strassner, U. Hintze, Chromatographia 50 (1999) 15.
[24] J.P. Vietzke, O. Brandt, D. Abeck, C. Rapp, M. Strassner, V. Schreiner, U. Hintze, Lipids 36 (2001) 299.
[25] T. Gildenast, J. Lasch, Biochim. Biophys. Acta 1346 (1997) 69.
[26] H. Farwanah, P. Nuhn, R.H.H. Neubert, K. Raith, Anal. Chim. Acta 492 (2003) 233–239.
[27] F. Bonte, P. Pinguet, J.M. Chevalier, A. Meybeck, J. Chromatogr. B 664 (1995) 311.
[28] M. Ponec, E. Boelsma, S. Gibbs, M. Mommaas, Skin Pharmacol. Appl. Skin Physiol. 15 (Suppl. 1) (2002) 4.
[29] A. Weerheim, M. Ponec, Arch. Dermatol. Res. 293 (2001) 191.
[30] Y. Uchida, M. Hara, H. Nishio, E. Sidransky, S. Inoue, F. Otsuka, A. Suzuki, P.M. Elias, W.M. Holleran, S. Hamanaka, J. Lipid Res. 41 (2000) 2071.
[31] K. Raith, J. Darius, R. Neubert, J. Chromatogr. A 876 (2000) 229.
[32] F.F. Hsu, J. Turk, M.E. Stewart, D.T. Downing, J. Am. Soc. Mass Spectrom. 13 (2002) 680.
[33] H. Farwanah, H. Wohlrab, R.H.H. Neubert, K. Raith, Anal. Bioanal. Chem. 383 (2005) 632–637.
[34] J. Reichelt, T. Doering, E. Schnetz, M. Fartasch, K. Sandhoff, A.M. Magin, J. Invest. Dermatol. 113 (1999) 329.
[35] P. Signorelli, Y.A. Hannun, Methods Enzymol. 345 (2002) 275.
[36] X. Han, Anal. Biochem. 302 (2002) 199.
[37] P.W. Wertz, D.C. Swartzendruber, K.C. Madison, D.T. Downing, J. Invest. Dermatol. 89 (1987) 419.
[38] D.C. Swartzendruber, P.W. Wertz, K.C. Madison, D.T. Downing, J. Invest. Dermatol. 88 (1987) 709.
[39] Y. Masukawa, H. Tsujimura, H. Narita, J. Lipid Res. 47 (2006) 1559.
[40] W.C. Byrdwell, R.H. Perry, J. Chromatogr. A 1133 (2006) 149.
[41] M. Ponec, A. Weerheim, P. Lankhorst, P. Wertz, J. Invest. Dermatol. 120 (2003) 581.
[42] J. Rogers, C. Harding, A. Mayo, J. Banks, A. Rawlings, Arch. Dermatol. Res. 288 (1996) 765.
[43] L. Norlén, I. Nicander, B. Lundh Rozell, S. Ollmar, B. Forslind, J. Invest. Dermatol. 112 (1999) 72.
[44] K. De Paepe, A. Weerheim, E. Houben, D. Roseeuw, M. Ponec, V. Rogiers, Skin Pharmacol. Physiol. 17 (2004) 23.